Application of an IE-Based Domain Decomposition Method for Analysis of Planar Microstrip Array Structures: Meshless Approach

B. Honarbakhsh [1] and A. Tavakoli [2,3]

[1] Department of Electrical Engineering
Shahid Beheshti University, Tehran, IRAN
b_honarbakhsh@sbu.ac.ir

[2] Department of Electrical Engineering
[3]Institute of Communications Technology and Applied Electromagnetics
Amirkabir University of Technology (Tehran Polytechnic), Tehran, IRAN
tavakoli@aut.ac.ir

Abstract **─** In this paper, application of an integral equation based domain decomposition method (DDM), developed for numerical solution of one-dimensional Fredholm integral equations of the second kind, is extended to electric field and mixed potential integral equations in two dimensions. Even though the original DDM was developed based on the Nyström method, results of the present work shows that meshfree approach can also be utilized. The extended DDM is employed for efficient meshfree analysis of planar microstrip array structures in the sense of reduced-size shape function and stiffness matrices. Results are validated by method of moments.

Index Terms **─** Array, domain decomposition, EFIE, meshfree, microstrip, MPIE.

I. INTRODUCTION

The purpose of Schwarz, when developed the domain decomposition method (DDM), was solution of boundary value problems over non-canonical domains [1]. Currently, this method follows diverse targets which the most famous of them is parallel processing [2]. In this application, the problem is decomposed to several smaller size problems and each of them is passed to a processor of a parallel processing architecture. DDMs are also a mean for hybridizing different numerical methods, where each domain of the problem is analyzed by its own proper numerical method [3]. The said two applications of DDMs are independent of numerical method(s) used for discretization of the original problem domain. Besides, DDMs are helpful in efficient solution of problems by meshfree methods (MFMs), at least, from two aspects. First, when using radial basis functions in a problem with large number of nodes, application of DDMs leads to several small size shape function matrices with relatively low order of condition numbers, which in turn, increases the efficiency of the interpolation process [4]. Second, noting to intrinsic deficiency of meshfree methods in handling problems with step-wise constitutive parameters, DDMs can be used to decouple different media and thus, significantly improve the efficiency of MFMs in the sense of convergence [5]. Currently, DDMs are mostly developed for solution of partial differential equations, with some few ones for integral equations [6-11]. It is worth mentioning that domain decomposition methods, regardless of their application, can be implemented in serial or parallel, especially, when the purpose of their application is not parallel processing.

In this paper, the DDM proposed in [11] is arranged for efficient meshfree solution of planar microstrip array structures in the sense of reduced-size shape function and stiffness matrices. This DDM is originally developed for numerical solution of one-dimensional Fredholm integral equations of the second kind based on the Nyström method. Results of the present work show that meshfree approach can also be utilized. The main claims of the present work are: first, the said DDM can be generalized to handle electric field integral equation (EFIE) and mixed potential integral equation (MPIE) in two dimensions. Second, it can be applied to the meshless collocation method and thus, its usage is not restricted to the Nyström method. It should be noted that this DDM is non-overlapping; therefore, it is best fitted to handle array structures.The results are validated by method of moments (MoM).

II. OVERVIEW OF THE OIRIGNAL IDEA

In this section, the DDM proposed in [11] is briefly introduced by considering the following IE:

$$\lambda u(x)+\int_{\Omega}u(x')K(x,x')dx'=f(x),\quad x\in\Omega, \tag{1}$$

where Ω, u, f, K and λ are, respectively, problem domain,

Submitted On: October 15, 2014
Accepted On: June 19, 2015

unknown function, excitation function, equation kernel and a scalar constant. Assume:

$$\begin{cases}\Omega=\Omega_1\bigcup\Omega_2\\ \Omega_1\bigcap\Omega_2=\varnothing\end{cases}. \tag{2}$$

This means that the problem domain is partitioned to two sub-domains. In addition, assume:

$$u(x)=\begin{cases}u_1(x), & x\in\Omega_1\\ u_2(x), & x\in\Omega_2\end{cases}. \tag{3}$$

Thus, (1) can be re-written as:

$$\begin{aligned}&\lambda u(x)+\int_{\Omega_1}u_1(x')K(x,x')dx'\\ &+\int_{\Omega_2}u_2(x')K(x,x')dx'\\ &=f(x),\quad x\in\Omega.\end{aligned} \tag{4}$$

As well, let:

$$f(x)=\begin{cases}f_1(x), & x\in\Omega_1\\ f_2(x), & x\in\Omega_2\end{cases}. \tag{5}$$

Therefore, solution of (1) can be obtained by solution of the following system of IEs [11]:

$$\begin{cases}\lambda u_1(x)+\int_{\Omega_1}u_1(x')K(x,x')dx'=h_1(x), & x\in\Omega_1\\ \lambda u_2(x)+\int_{\Omega_2}u_2(x')K(x,x')dx'=h_2(x), & x\in\Omega_2\end{cases}, \tag{6}$$

where:

$$\begin{cases}h_1(x)=f_1(x)-\int_{\Omega_2}u_2(x')K(x,x')dx', & x\in\Omega_1\\ h_2(x)=f_2(x)-\int_{\Omega_1}u_1(x')K(x,x')dx', & x\in\Omega_2\end{cases}, \tag{7}$$

which states that solution of (1) over Ω can be found by solution of (6) wherein, its first equation is over Ω_1, only, and its second equations is over Ω_2, only. Numerical solution of the (6) can be obtained iteratively by choosing $u_1^{(0)}$ as an initial guess for u_1 and evaluating its value at the kth iteration from:

$$\begin{cases}h_2^{(k-1)}(x)=f_2(x)\\ \quad-\int_{\Omega_1}u_1^{(k-1)}(x')K(x,x')dx', \quad x\in\Omega_2\\ \lambda u_2^{(k-1/2)}(x)+\int_{\Omega_2}u_2^{(k-1/2)}(x')K(x,x')dx'\\ \quad=h_2^{(k-1)}(x), \quad x\in\Omega_2\\ h_1^{(k-1/2)}(x)=f_1(x)\\ \quad-\int_{\Omega_2}u_2^{(k-1/2)}(x')K(x,x')dx', \quad x\in\Omega_1\\ \lambda u_1^{(k)}(x)+\int_{\Omega_1}u_2^{(k)}(x')K(x,x')dx'\\ \quad=h_1^{(k-1/2)}(x), \quad x\in\Omega_1\end{cases}, \tag{8}$$

for k = 1, 2, …. The solution can also be computed by starting from an initial guess for u_2. Extension of the method to more sub-domains is straightforward.

III. GENERALIZATION OF THE ORIGINAL DDM TO 2D-EFIE AND 2D-MPIE

The formulation reported in this section is restricted to planar microstrip structure. Consider two equi-plane non-overlapping microstrip circuits as depicted in Fig. 1. The global domain and perimeter of the structure are Ω and $\partial\Omega$, respectively (not shown in the figure). Unit normal vectors to Ω and $\partial\Omega$ are $\mathbf{n}$ (normal to the paper) and $\mathbf{m}$, respectively. It is assumed that the structure is perfect electric conductor, placed on the *xy* plane and is excited by the field $\mathbf{E^i}$, which induces the surface current density $\mathbf{J_s}$ on the conductors.

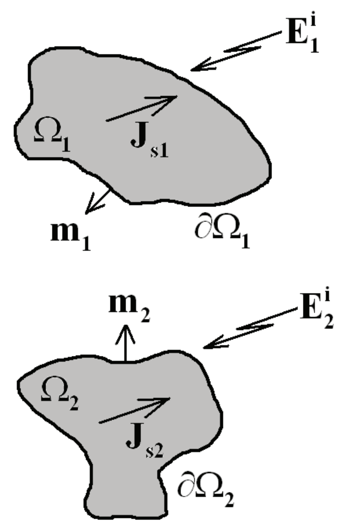

Fig. 1. Two equi-plane non-overlapping microstrip circuits.

Equations governing $\mathbf{J_s}$ in the EFIE and MPIE formulations are:

$$\begin{cases}\mathbf{n}\times O\left[\mathbf{J}_s(\boldsymbol{\rho})\right]=\mathbf{n}\times\mathbf{E}^i(\boldsymbol{\rho}), & \boldsymbol{\rho}\in\Omega\\ \mathbf{m}\cdot\mathbf{J}_s(\boldsymbol{\rho})=0, & \boldsymbol{\rho}\in\partial\Omega\end{cases}, \tag{9}$$

with:

$$O(\cdot)=\begin{cases}j\omega\mu_0\left(1+k_0^{-2}\nabla\nabla\cdot\right)\int_\Omega\overline{\overline{\mathbf{G}}}_A(\boldsymbol{\rho},\boldsymbol{\rho}')\cdot(\cdot)\mathrm{d}\Omega, \quad \text{2D-EFIE}\\ j\omega\mu_0\int_\Omega\overline{\overline{\mathbf{G}}}_A(\boldsymbol{\rho},\boldsymbol{\rho}')\cdot(\cdot)\mathrm{d}\Omega\\ \quad-(j\omega\varepsilon_0)^{-1}\nabla\int_\Omega G_V(\boldsymbol{\rho},\boldsymbol{\rho}')\nabla'\cdot(\cdot)\mathrm{d}\Omega, \quad \text{2D-MPIE}\end{cases}, \tag{10}$$

where $\overline{\overline{\mathbf{G}}}_A$ and G_V are dyadic and scalar Green's function of the microstrip substrate, respectively [12]. Following the previous section, let:

$$\mathbf{J}_s=\begin{cases}\mathbf{J}_{s1}, & \boldsymbol{\rho}\in\Omega_1\\ \mathbf{J}_{s2}, & \boldsymbol{\rho}\in\Omega_2\end{cases}, \tag{11}$$

and

$$\mathbf{m} = \begin{cases} \mathbf{m}_1, & \boldsymbol{\rho} \in \partial\Omega_1 \\ \mathbf{m}_2, & \boldsymbol{\rho} \in \partial\Omega_2 \end{cases}, \tag{12}$$

and

$$\mathbf{E}^{\mathbf{i}} = \begin{cases} \mathbf{E}_1^{\mathbf{i}}, & \boldsymbol{\rho} \in \Omega_1 \\ \mathbf{E}_2^{\mathbf{i}}, & \boldsymbol{\rho} \in \Omega_2 \end{cases}, \tag{13}$$

and

$$\begin{cases} \mathbf{h}_1(\boldsymbol{\rho}) = \mathbf{E}_1^{\mathbf{i}}(\boldsymbol{\rho}) - O\left[\mathbf{J}_{\mathbf{s2}}(\boldsymbol{\rho})\right], & \boldsymbol{\rho} \in \Omega_1 \\ \mathbf{h}_2(\boldsymbol{\rho}) = \mathbf{E}_2^{\mathbf{i}}(\boldsymbol{\rho}) - O\left[\mathbf{J}_{\mathbf{s1}}(\boldsymbol{\rho})\right], & \boldsymbol{\rho} \in \Omega_2 \end{cases}. \tag{14}$$

Thus, taking initial guess for $\mathbf{J}_{\mathbf{s1}}$, unknown current densities $\mathbf{J}_{\mathbf{s1}}$ and $\mathbf{J}_{\mathbf{s2}}$ can be iteratively found from:

$$\begin{cases} \mathbf{h}_2^{(k-1)}(\boldsymbol{\rho}) = \mathbf{E}_2^{\mathbf{i}}(\boldsymbol{\rho}) - O\left[\mathbf{J}_{\mathbf{s1}}^{(k-1)}(\boldsymbol{\rho})\right], & \boldsymbol{\rho} \in \Omega_2 \\ \begin{cases} \mathbf{n} \times O\left[\mathbf{J}_{\mathbf{s2}}^{(k-1/2)}(\boldsymbol{\rho})\right] = \mathbf{n} \times \mathbf{h}_2^{(k-1)}(\boldsymbol{\rho}), & \boldsymbol{\rho} \in \Omega_2 \\ \mathbf{m}_2 \cdot \mathbf{J}_{\mathbf{s2}}^{(k-1/2)}(\partial\Omega_2) = 0, \end{cases} \\ \mathbf{h}_1^{(k-1/2)}(\boldsymbol{\rho}) = \mathbf{E}_1^{\mathbf{i}}(\boldsymbol{\rho}) - O\left[\mathbf{J}_{\mathbf{s2}}^{(k-1/2)}(\boldsymbol{\rho})\right], & \boldsymbol{\rho} \in \Omega_1 \\ \begin{cases} \mathbf{n} \times O\left[\mathbf{J}_{\mathbf{s1}}^{(k)}(\boldsymbol{\rho})\right] = \mathbf{n} \times \mathbf{h}_1^{(k-1/2)}(\boldsymbol{\rho}), & \boldsymbol{\rho} \in \Omega_1 \\ \mathbf{m}_1 \cdot \mathbf{J}_{\mathbf{s1}}^{(k-1/2)}(\partial\Omega_1) = 0, \end{cases} \end{cases}, \tag{15}$$

for $k = 1, 2, \ldots$.

IV. NUMERICAL RESULTS

In this section, the generalized DDM is applied to three microstrip array structures. The meshfree collocation method proposed in [13] is used for discretization of the problem domains. Results obtained from the first two structures are compared with the Agilent® Momentum® 2009, and result of the last one is validated by FEKO® suite 5.5. Convergence curves corresponding to DDM are generated based on relative error of successive iterations, defined by:

$$r_e^{(k)} = \left\| u^{(k+1)} - u^{(k)} \right\| / \left\| u^{(k)} \right\|, \tag{16}$$

where $\| u \| = \left(\int_\Omega |u|^2 \, d\Omega \right)^{1/2}$.

A. Two-element array

This structure consists of two line-fed patch antennas, placed vertically apart each other at distance d, as depicted in Fig. 2. Each array element is a line-fed patch antenna, similar to one introduced in [13]. The excited element is the element number one. For investigating the effect of different parameters on the convergence trend, the array is analyzed for two different vertical offsets; *i.e.*, d = 20 and 2.5 mm. Simulated S-parameter of the excited element at d = 20 mm is reported in Fig. 3.

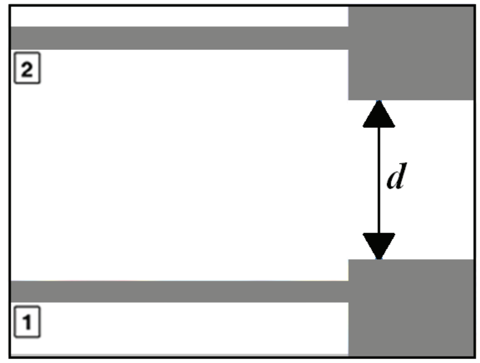

Fig. 2. Arrangement of the two-element array.

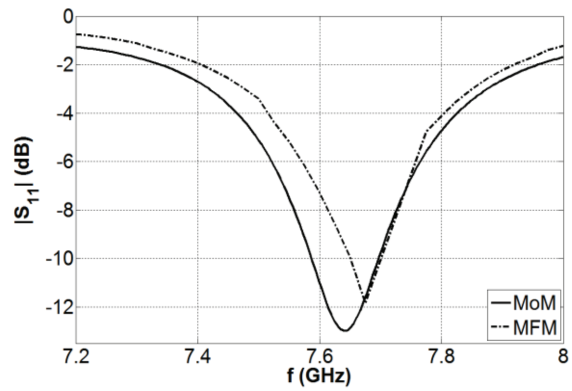

Fig. 3. Two-element array: $|S_{11}|$ at d = 20 mm.

The effect of initial guess on convergence is reported in Fig. 4, where analysis is performed at the antenna resonance frequency; *i.e.*, 7.675 GHz. It can be observed that the convergence is affected by the initial guess. However, the overall convergence of the method seems to be independent of it. The zero-valued initial vector shows faster convergence. Thus, hereafter, all initial guesses will be taken to be zero.

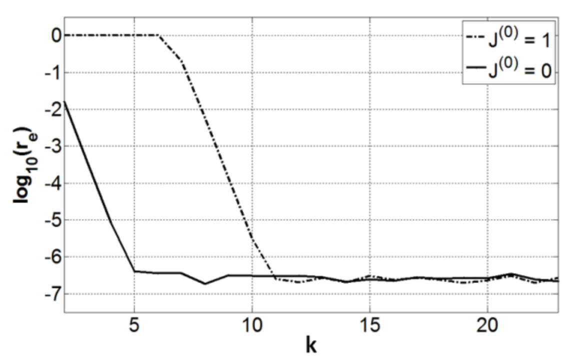

Fig. 4. Two-element array: effect of initial guess on DDM convergence at d = 20 mm.

The current distribution over the elements at $d = 20$ mm are reported in Fig. 5, wherein for better visualization of the coupling effect, it is also depicted in logarithmic scale.

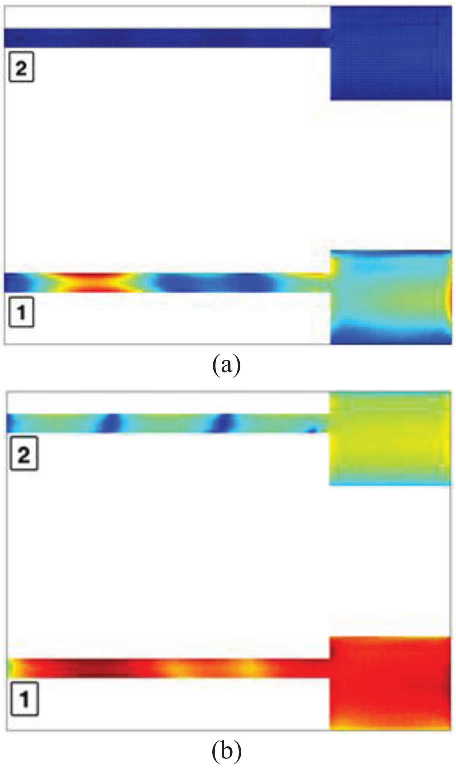

Fig. 5. Two-element array: current distribution at $d = 20$ mm: (a) linear scale, (b) logarithmic scale.

To study the effect of element coupling on the convergence, the array is analyzed at 2.5 mm distance, which ensures considerable EM interaction. The S-parameter of the exited element and its corresponding convergence curves are reported in Figs. 6 and 7, respectively.

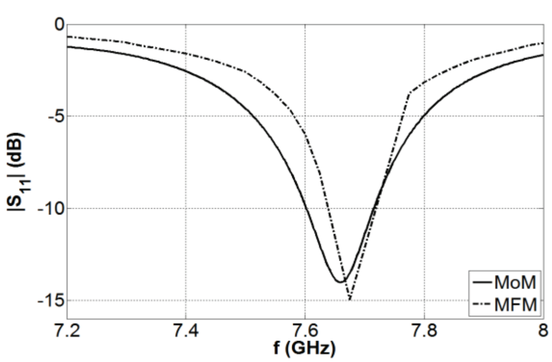

Fig. 6. Two-element array: $|S_{11}|$ at $d = 2.5$ mm.

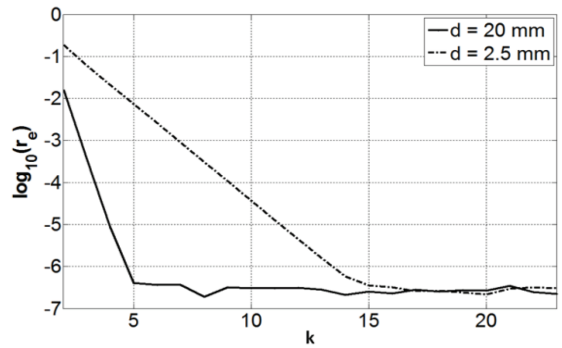

Fig. 7. Two-element array: effect of initial guess on DDM convergence at $d = 2.5$ mm.

As can be predicted, increase in the amount of coupling, defers the convergence of the method. As in the previous case, the current distributions are depicted in Fig. 8.

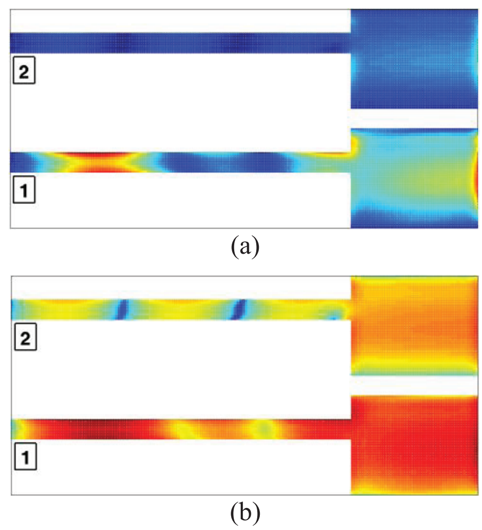

Fig. 8. Two-element array: current distribution at $d = 2.5$ mm: (a) linear scale, (b) logarithmic scale.

B. Four-element array

This array is composed from four line-fed patch antennas in a cross arrangement with $d = 8$ mm inter-element spacing. Each element of this structure is a square patch antenna with 16 mm side length, fed by a microstrip line of 2.5 mm width. The transmission line is placed 8.5 mm apart from the corner of each patch. Relative electric permittivity and thickness of the microstrip substrate are taken to be 2.2 and 0.794 mm, respectively. The arrangement of the array is depicted in Fig. 9. The excited element is again, the element number one. Such a structure can be used for generation of circular polarized waves [14].

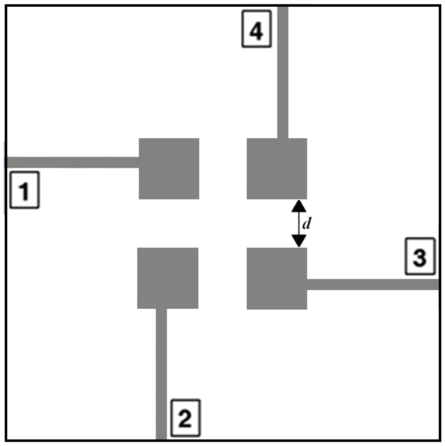

Fig. 9. Arrangement of the four-element array.

Simulated S-parameter of the excited element is reported in Fig. 10. Effect of frequency on convergence is reported in Fig. 11, wherein $f = 8.4$ GHz represents the situation which the delivered EM energy to the patch is negligible and $f = 8.825$ GHz, the antenna resonance frequency, is the frequency that the input EM energy is maximum. As can be seen, convergence of the method is deferred at the resonance frequency. The current distribution at resonance is depicted in Fig. 12.

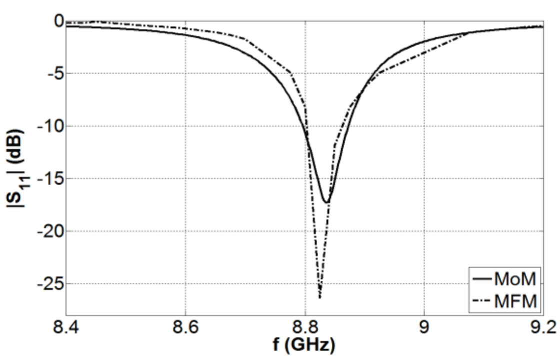

Fig. 10. Four-element array: $|S_{11}|$.

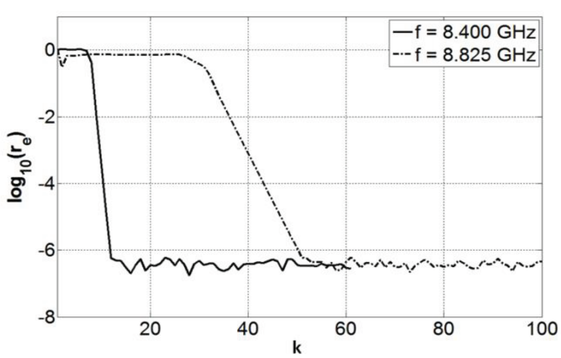

Fig. 11. Four-element array: effect of frequency on DDM convergence.

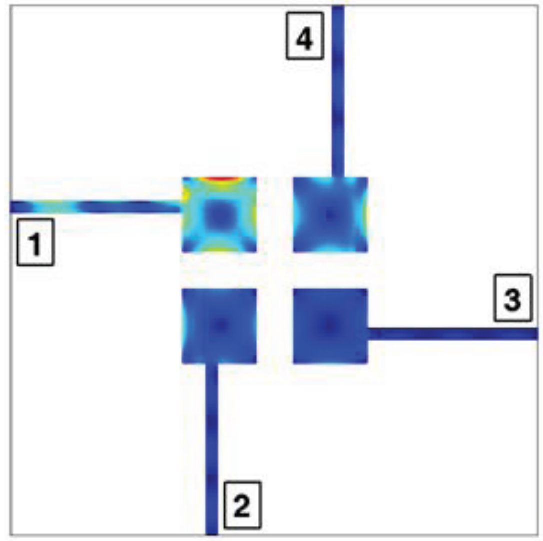

(a)

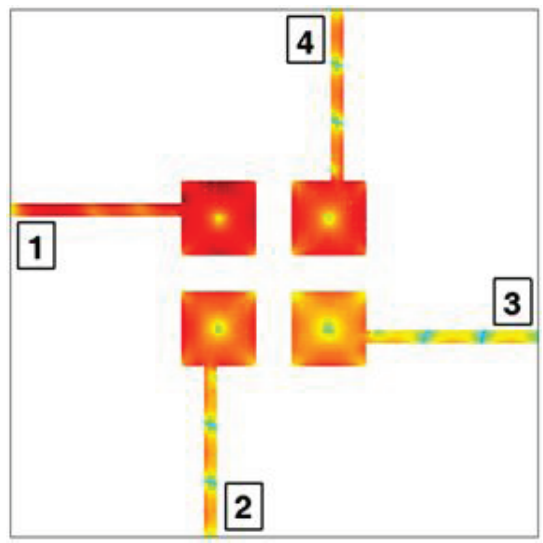

(b)

Fig. 12. Four-element array: current distribution at resonance: (a) linear scale, (b) logarithmic scale.

C. 225 element array

The last analyzed structure is a 225 element array of $\lambda/2$ square patches, suspended $\lambda/10$ above an infinite ground plane, where λ is the working wavelength. The patches are placed in a 15×15 square arrangement with $\lambda/2$ inter-element spacing. An equivalent microstrip substrate for this case has unit electric permittivity and thus, its analysis can be performed based on the EFIE formulation. This array is illuminated by a plane wave at sixty degree angle with respect to the array normal direction. The corresponding normalized scattered field and convergence curve are depicted in Figs. 13 and 14, respectively. The current distributions over the nine central elements are depicted in Fig. 15.

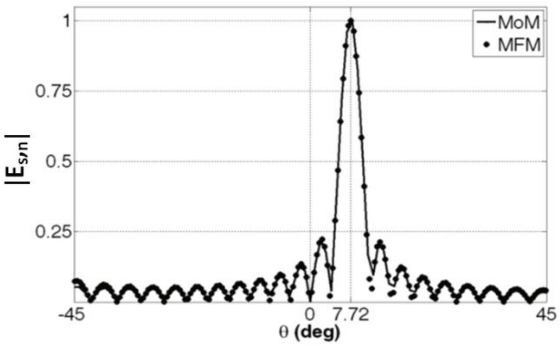

Fig. 13. 225 element array: normalized scattered field.

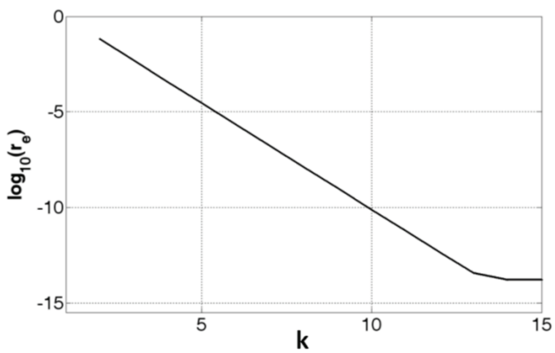

Fig. 14. 225 element array: DDM convergence curve.

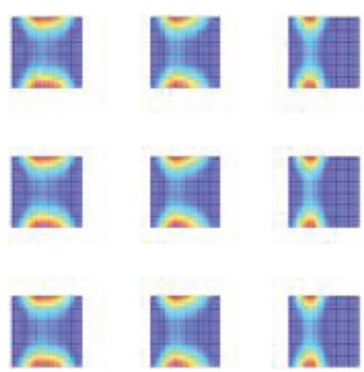

Fig. 15. 225 element array: current distribution over the nine central elements.

V. CONCLUSION

In this work, it is shown that the application of the domain decomposition method, developed for numerical solution of one-dimensional Fredholm integral equations of the second kind with Nyström discretization, can be extended for efficient meshfree analysis of planar microstrip array structures. Both of the EFIE and MPIE formulations are considered. The initial guess can affect the convergence trend, although the overall convergence seems to be independent of it. The increase of EM coupling between the elements defers the convergence of the method. The same behavior is observed when the frequency of the analysis approaches the resonance frequency of the structure. The results are validated by method of moments.

ACKNOWLEDGMENT

The authors appreciate Prof. M. Dehghan for inputs regarding meshfree methods and Dr. R. Mirzavand for inputs regarding domain decomposition methods.

REFERENCES

[1] H. A. Schwarz, "Uber einige abbildungsaufgaben," *Ges. Math. Abh.*, vol. 70, pp. 105-120, 1869.

[2] Domain Decomposition Methods in Science and Engineering, 1-12, *Proc. Int. Conf.*, *SIAM*, *AMS*, John Wiley & Son, DD Press, 1987-1999.

[3] C. Carstensen, M. Kuhn, and U. Langer, "Fast parallel solvers for symmetric boundary element domain decomposition methods," *Numer. Math.*, vol. 79, pp. 321-347, 1998.

[4] R. Schaback, "Error estimates and condition numbers for radial basis function interpolation," *Adv. Comput. Math.*, vol. 3, pp. 251-264, 1995.

[5] T. Kaufmann, "The meshless radial point interpolation method for electromagnetics," *Doctoral and Habilitation Theses*, ETH, 2011.

[6] Z. Peng, X. C. Wang, and J. F. Lee, "Integral equation based domain decomposition method for solving electromagnetic wave scattering from non-penetrable objects," *IEEE Trans. Antennas Propag.*, vol. 59, no. 9, pp. 3328-3338, 2011.

[7] J. Hu, W. Hong, H. X. Zhou, W. D. Li, and Z. Song, "An overlapped domain decomposition method for solving electromagnetic surface integral equations," *IEEE Int. Conf. Comput. Problem-Solving* (*ICCP*), pp. 1-4, 2010.

[8] E. P. Stephan and T. Tran, "Domain decomposition algorithms for indefinite hypersingular integral equations: the *h* and *p* versions," *SIAM J. Sci. Comput.*, vol. 19, no. 4, pp. 1139-1153, 1998.

[9] W. D. Li, W. Hong, and H. X. Zhou, "Integral equation-based overlapped domain decomposition method for the analysis of electromagnetic scattering of 3D conducting objects," *Microwave Opt. Tech. Lett.*, vol. 49, no. 2, pp. 265-274, 2007.

[10] P. Ylä-Oijala, V. Lancellotti, B. P. de Hon, and S. Järvenpää, "Domain decomposition methods combining surface equivalence principle and macro basis functions," *ACES J.*, vol. 25, no. 12, pp. 1017-1025, 2010.

[11] M. Campos and C. E. Perez, "A domain decomposition scheme for Fredholm integral equations using Nyström discretization," *Technical Report 98-21*, Departamento de Ingenieria Matematica, Universidad de Concepcion, 1998.

[12] J. R. Mosig, "Arbitrarily shaped microstrip structures and their analysis with a mixed potential

integral equation," *IEEE Trans. Microwave Theory Tech.*, vol. MTT-36, pp. 314-323, 1988.

[13] B. Honarbakhsh and A. Tavakoli, "Analysis of thick microstrip antennas by meshfree collocation method," *ACES J.*, vol. 28, no. 2, pp. 99-109, 2013.

[14] P. S. Hall, "Review of techniques for dual and circularly polarized microstrip antennas," in *Microstrip Antennas, the Analysis and Design of Microstrip antennas and Arrays*, D. M. Pozar and D. H. Schaubert, IEEE Press, pp. 107-116, 1995.

B. Honarbakhsh born in Tehran, Iran, in 1981. He received his B.S., M.S. and Ph.D. degrees in Electrical Engineering, all from Amirkabir University of Technology, in 2004, 2007 and 2012. He is currently an Assistant Professor in the Department of Electrical Engineering at Shahid Beheshti University. His research interest is numerical electromagnetics.

Ahad Tavakoli was born in Tehran, Iran, on March 8, 1959. He received his B.S. and M.S. degrees from the University of Kansas, Lawrence, and the Ph.D. degree from the University of Michigan, Ann Arbor, all in Electrical Engineering, in 1982, 1984, and 1991, respectively. He is currently a Professor in the Department of Electrical Engineering at Amirkabir University of Technology. His research interests include EMC, scattering of electromagnetic waves and microstrip antennas.